國立交通大學

電子工程系　　　電子研究所碩士班

碩 士 論 文

結構不完美在自組性砷化銦奈米環的反磁性能量

位移之影響：以理論計算方法

Effect of Structural Imperfections on the Excitonic Energy
Diamagnetic Shift on Self-assembled *InAs/GaAs* Nano-rings :
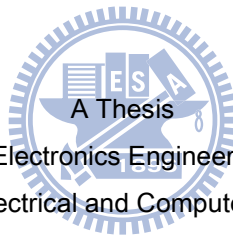A Theoretical Approach

研 究 生：邱偉庭

指導教授：霍斯科　教授

中華民國九十九年十一月

結構不完美在自組性砷化銦奈米環的
反磁性能量位移之影響：以理論計算方法
Effect of Structural Imperfections on the Excitonic Energy Diamagnetic
Shift in Self-assembled *InAs/GaAs* Nano-rings :
A Theoretical Approach

研 究 生：邱偉庭　　　　Student：Wei-ting Chiu
指導教授：霍斯科　　　　Advisor：Oleksandr Voskoboynikov

國 立 交 通 大 學
電 子 工 程 學 系 電 子 研 究 所
碩 士 論 文

A Thesis
Submitted to Department of Electronics Engineering and Institute of electronics
College of Electrical and Computer Engineering
National Chiao Tung University
in partial Fulfillment of the Requirements
for the Degree of
Master
in

Electronics Engineering

November 2010

Hsinchu,　Taiwan, Republic of China

中華民國九十九年十一月

結構不完美在自組性砷化銦奈米環的

反磁性能量位移之影響：以理論計算方法

學生：邱偉庭　　　　　　　　　　　　　　　　指導教授：霍斯科

國立交通大學

電子工程學系　電子研究所碩士班

摘　要

　　在這份研究裡，我們使用映像法以及直接對角化法來計算激子在自組性半導體量子環的反磁性能量位移。映像法能夠在三維空間中描述該量子環的物質特性，而直接對角化法則提供了一個途徑來計算激子的能量以及波函數。我們從一個環緣上對稱地上下搖擺的量子環開始研究，該量子環有著鏡像對稱的位能。接著我們考慮結構上的不完美，我們假設這些不完美是由不對稱的環緣上搖擺以及由不平衡的位能造成的，鏡像對稱也因此消失。我們的模擬結果顯示，只要很小的結構上不完美會使激子的波函數掉到其中一個位能谷裡，且波函數的分布範圍大量的縮減。激子的反磁性能量位移也大量的變小因為反磁性能量位移正比於激子波函數的分布範圍。我們計算得到的激子激態能量以及反磁性能量位移都與實驗上測量到的數據吻合。
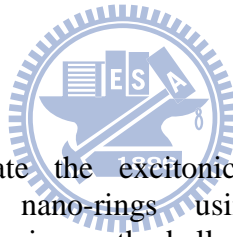
Effect of Structural Imperfections on the Excitonic Energy Diamagnetic
Shift in Self-assembled *InAs/GaAs* Quantum Rings :
A Theoretical Approach

Student: Wei-ting Chiu   Advisor: Prof. Voskoboynikov

Department of Electronics Engineering and
Institute of Electronics
National Chiao Tung University

ABSTRACT

In this study we calculate the excitonic energy diamagnetic shifts in self-assembled semiconductor nano-rings using the mapping and exact diagonalization methods. The mapping method allows a three dimensional description of the ring and the exact diagonalization method gives a way to compute the excitonic energies and wave functions. We start from symmetrically wobbled quantum rings with the electronic confinement potentials possessing a reflectional symmetry on the (110) plane. The structural imperfections are considered by applying small variations on the geometry and potential profile and thus the reflectional symmetry is broken. Our results show that with small structural imperfections the excitonic wave functions will be located in one of the potential valleys and the extension of the wave functions will shrink greatly. A dramatical decrease in the excitonic energy diamagnetic shift is observed because the diamagnetic shift depends on the effective area spanned by the excitonic wave function. The calculated excitonic ground state energies and diamagnetic shift coefficients are in good agreement with the experimental measurements.

誌　　　謝

　　這篇論文得以完成要感謝的人實在太多。首先必須感謝我的指導老師霍斯科教授，從大三下到碩士畢業這段期間，他在物理上的敏銳直覺解決了許多我在研究上的疑問，在寫作上，他更一一的指出我常犯的錯誤並加以修正，讓這篇論文的文字更加通順，而他也是一位很好的人生導師，教了我許多關於這個世界的知識。李建平老師在物理方面有很高的造詣，在量子力學的課堂裡，李老師灑脫且自信的寫下一條條物理方程式，而台下的我只有讚嘆的份。顏順通老師做事十分嚴謹，研究所修顏老師的電磁學以及固態物理課程時，他總是一絲不苟的推導出課本裡的式子，讓我很扎實的學到這些基礎物理理論。感謝上述三位老師擔任我的口試委員，對我的論文提出許多的建議，更讓我能夠從各個角度去思考。還要感謝實驗室的學長，Thu，對我的照顧，許多在論文寫作還有理論方面的討論對我有很大的幫助，林大鈞學長在實驗以及模擬上清楚的解釋讓我更快的對研究有所了解，實驗室的其他成員也讓我在研究生活不至於太孤獨。從大學到研究所這對期間，管絃樂社以及足球系隊是我在埋首書籍以及研究外最好的去處，修習音樂總是能夠讓心情放鬆，而運動鍛鍊出來的體力讓我能應付研究的壓力，也謝謝裡面所有的成員，讓我的生活不會枯燥乏味。感謝台南一中校友管樂團的成員讓我在讀書研究外有另一個小天地。感謝大學以及研究所的室友們，一起度過辛苦的實驗、煎熬的考試以及快樂的日子。感謝在新竹的親戚，給我生活上直接的援助。感謝徐若嵐一直在身邊陪伴我。最後要感謝我的父母邱文淵及吳秀瓊讓我能夠衣食無缺，無後顧之憂的進行研究。其他還有許多在這段期間曾幫助過我的人，雖無法一一細數，但還是從內心感謝你們助我順利完成學業。

Contents

i

List of Figures

List of Tables

Chapter 1

Introduction

In classical physics the magnetic response of a charged system is defined by the Lorentz force. Within the quantum domain the magnetic response of a ring structure shows an extraordinary result - the Aharonov-Bohm (AB) effect [1]. In some experiments the AB effect was clearly shown in the electronic energy spectra [2, 3] where magnetic dependent oscillations in the conductance and ground state energy were observed. Beside the experimental studies there were also theoretical investigations on the magnetic response of quantum-rings [4,5]. The magneto-optical properties of semiconductor nano-rings have called a considerable attention since the AB effect is not expected here because of the neutrality of exciton.

Recently, nano-ring structures were produced [8] and the magneto-excitonic ground-state behavior of a single quantum ring was observed [9]. According to the cross-sectional scanning-tunneling microscopy (X-STM) observations [8] those quantum rings are anisotropic in the height of the rim. Ring rim height in [110] direction is larger than in [1$\bar{1}$0]. Also a mathematical description of the geometry was suggested. Although there is no longer a rotational symmetry within this model, an inherent reflectional symmetry on the (110) plane exists. However, even there is still a reflectional symmetry, when calculating the excitonic energy the separation of variables is impossible. Hence, the excitonic energy can be simulated on the base of a three dimensional description.

In this study we investigate the excitonic ground state energy and diamagnetic shift for quantum nano-rings and compare our results with the experimental measurements [9]. We should note that the diamagnetic shift coefficient [10,11] indicates the area spanned by the wave function of a particle confined to a system. In our simulation we found that the mathematical model with reflectional symmetry on the (110) plane would make the exciton wave function

1

equally distributed into the two potential valleys of the quantum ring's potential. Nevertheless, the perfect reflectional symmetry of the system only exists in idealized mathematical model and there would always be some structural imperfections which break the reflectional symmetry. Therefore, to include the imperfections in the model we made adjustments for both the geometry and confinement potential of the quantum rings. Changing the height profile on one of the wobbled hills causes a wobbling asymmetry on the quantum ring, and a disbalanced potential is resulted in the different depths of one of the side potential valleys. Our result shows that with small deviations in the height profile and confinement potential on one side (the positive x side) of the ring, the distribution of the excitonic wave function would collapse into the corresponding potential valley, causing a drop on the excitonic energy diamagnetic shift coefficient.

This report is organized as follows: in chapter two we describe nano-ring systems in their geometry and confinement potentials, including structural imperfections into the mathematical model, and the simulation method is presented; the simulation results are discussed in chapter three; finally, we summarize our work and propose possible future works.
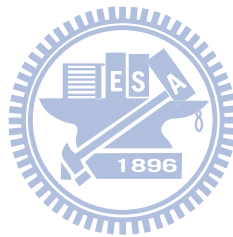
Chapter 2

Theory

2.1 Description of the System

To build a model of a quantum ring, we first assume that the ring is grown on a plane parallel to the x-y plane and an external magnetic field applied in z-direction. The height profile of the ring is taken from Ref. [12] which fits actual shape of a quantum ring. We modify it in order to apply in this study a wobbling asymmetry:

$$
\begin{aligned}
h(x, y) &= h_0 + [1 + a_{in} \cdot C(x, y)] \cdot \frac{\left[\widetilde{h}_M(x, y) - h_0\right] \widetilde{\gamma}_0(x, y)^2}{\Delta R(x, y)^2 + \widetilde{\gamma}_0(x, y)^2} \cdot \frac{\widetilde{R}(x, y)^2 - \Delta R(x, y)^2}{\widetilde{R}(x, y)^2}, \\
&\quad \sqrt{x^2 + y^2} \leq \widetilde{R}; \\
h(x, y) &= h_\infty + [1 + a_{out} \cdot C(x, y)] \cdot \frac{\left[\widetilde{h}_M(x, y) - h_\infty\right] \widetilde{\gamma}_\infty(x, y)^2}{\Delta R(x, y)^2 + \widetilde{\gamma}_\infty(x, y)^2}, \quad \sqrt{x^2 + y^2} > \widetilde{R},
\end{aligned}
$$

(2.1)

where

$$
C(x, y) = \exp\left[-\frac{(x - x_p)^2 + (y - y_p)^2}{b^2}\right],
$$

(2.2)

$$
\widetilde{h}_M(x, y) = h_M\left(1 + \xi\frac{x^2 - y^2}{x^2 + y^2}\right),
$$

(2.3)

$$
\widetilde{R}(x, y) = R\left(1 + \xi_R\frac{x^2 - y^2}{x^2 + y^2}\right),
$$

(2.4)

$$
\Delta R(x, y) = \sqrt{x^2 + y^2} - \widetilde{R},
$$

(2.5)

$$
\widetilde{\gamma}_0(x, y) = \gamma_0\left(1 + \xi_\gamma\frac{x^2 - y^2}{x^2 + y^2}\right),
$$

(2.6)
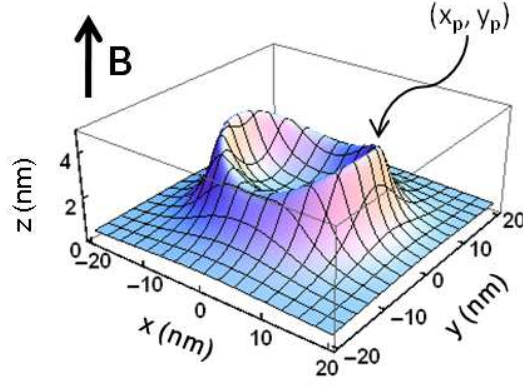
Figure 2.1: Geometry of a symmetrically wobbled nano-ring with uniform magnetic field applied in z-direction.

$$\widetilde{\gamma}_{\infty}(x,y) = \gamma_{\infty}\left(1 + \xi_{\gamma}\frac{x^2 - y^2}{x^2 + y^2}\right). \tag{2.7}$$

The parameters (x_p, y_p) indicate the ring's peak positions on the rim (see fig. 2.1, as the arrow pointed), b controls the range of wobbling asymmetry, a_{in} and a_{out} can be manipulated to give different degree of wobbling asymmetries, and R is the radius of the rim. If $a_{in} = a_{out} = 0$ the ring has a reflectional symmetry about x=0 plane and the wobbling is symmetric (see fig. 2.1 and Ref. [12]).

Using this geometry we create a corresponding electronic confinement potential:

$$V_e(x,y,z) = \Delta E \cdot \left\{1 - \frac{1 + \tanh\left(\frac{z}{a}\right)}{2} \cdot \left[1 - \frac{1 + \tanh\left(\frac{z - h(x,y)}{a}\right)}{2}\right]\right\}. \tag{2.8}$$

This expression gives a slowly changing potential for electron confined in the ring which reflects the composition of *InAs* smoothly varying from inside (the ring's indium-rich part) to outside.

From Fig. 2.2 it should noticed that unlike a conventional doubly-connected ring, this structure is singly-connected since the center is not hollow. However, it still possesses some ring's properties since the probability density of the exciton confined inside the ring, at the rim position is still higher than at the center part, thus it is a ring-like nano structure.

We assume that there are two reasons for the structural imperfections. The first one comes from a wobbling asymmetry of the height profile of the nano-ring. We can achieve such geom-

4

Figure 2.2: Contour plot of the electronic confinement potential of a symmetrically wobbled ring. The potential is projected onto (a) the x-z plane and (b) the y-z plane.

etry imperfections (wobbling asymmetry) by substituting different values of a_{in} and a_{out}. We define the degree of the wobbling asymmetry Δh on the rim of the ring by
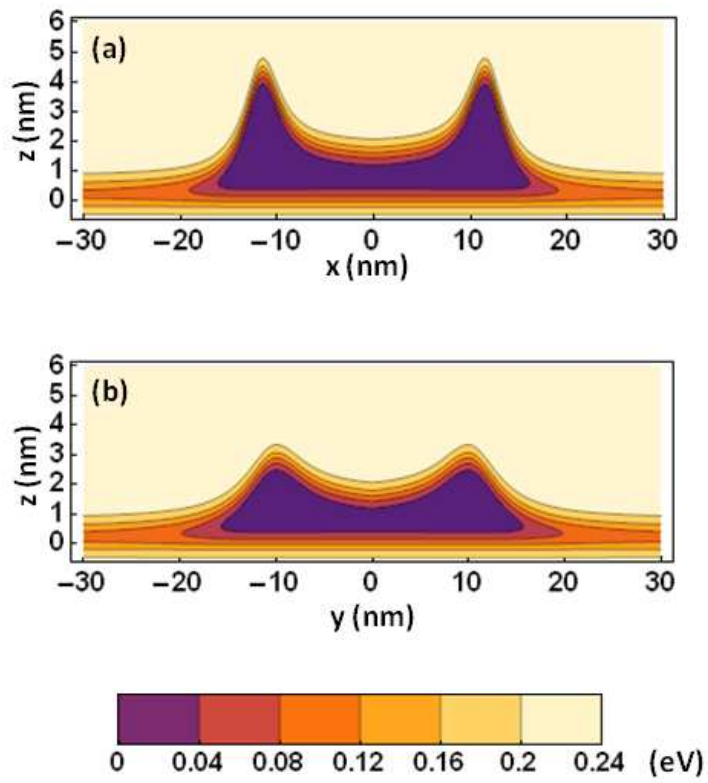
$$\Delta h = \frac{h_+ - h_-}{h_-} \times 100\%, \tag{2.9}$$

where $h_+(h_-)$ indicate the height at the peak's positions on the rim in the +(-) x-direction. A set of parameters $\{a_{in}, a_{out}\}$ gives a value of Δh.

Another origin of the structural imperfections is disbalanced potential valley depths along x-axis. To model the potential depth change on the positive x-side we define another expression for the electronic confinement potential

$$\begin{aligned}
V_e(x,y,z) &= \Delta E \cdot \left\{ 1 - \frac{1 + \tanh\left(\frac{z}{a}\right)}{2} \cdot \left[1 - \frac{1 + \tanh\left(\frac{z - h(x,y)}{a}\right)}{2} \right] \right\} \\
&\quad \cdot \left\{ \left(1 - \frac{1 + \tanh\left(\frac{x - b_V}{b_V}\right)}{2} \right) + \left(1 - \frac{1 + \tanh\left(\frac{x_V - x}{b_V}\right)}{2} \right) \right\} \\
&\quad + \Delta E \cdot \left\{ 1 - (1 + \Delta V) \cdot \frac{1 + \tanh\left(\frac{z}{a}\right)}{2} \cdot \left[1 - \frac{1 + \tanh\left(\frac{z - h(x,y)}{a}\right)}{2} \right] \right\} \\
&\quad \cdot \left(1 - \frac{1 + \tanh\left(\frac{x - b_V}{b_V}\right)}{2} \right) \cdot \left(1 - \frac{1 + \tanh\left(\frac{x_V - x}{b_V}\right)}{2} \right),
\end{aligned} \tag{2.10}$$

where x_V and b_V controls the range of the disbalanced potential, and ΔV indicates the value of disbalance. The potential on the negative x-side is unchanged.

The value ΔV reflects the indium composition (c of $In_c Ga_{1-c} As$) difference along x-direction. We can set $\Delta V = 0.1$ when the composition at the peak position at the rim of the ring on the positive x-direction is 10% more than on the negative x side. By varying Δh and ΔV we build a model of nano-rings with two kinds of structural imperfections: the wobbling asymmetry in the geometry and disbalanced confinement potential.

2.2 Mapping Method

In order to have a unified parameter following the geometry and composition changes we define the mapping function [14] as follows:

$$M(x, y, z) = 1 - \frac{V_e(x, y, z)}{\Delta E_e}. \tag{2.11}$$

Using this function we can further obtain other position-dependent material parameters by the following interpolations:

$$
\begin{aligned}
m_{e(h)}^*(x, y, z) &= m_{e(h),in}^* \cdot M(x, y, z) + m_{e(h),out}^* \cdot \left[1 - M(x, y, z)\right], \tag{2.12}\\
\epsilon(x, y, z) &= \epsilon_{in} \cdot M(x, y, z) + \epsilon_{out} \cdot \left[1 - M(x, y, z)\right],\\
E_g(x, y, z) &= E_{g,in} \cdot M(x, y, z) + E_{g,out} \cdot \left[1 - M(x, y, z)\right],
\end{aligned}
$$

where $m_{e(h)}^*$ is the electron (hole) effective mass, ϵ is the permittivity, and E_g is the energy gap. The subscription of *in* and *out* indicate the corresponding inside (*InAs*) and the outside (*GaAs*) material parameters.

The hole confinement potential can be obtained from the electronic potential and the energy gap:

$$V_h(x, y, z) = E_g(x, y, z) - V_e(x, y, z) - E_{g,in}. \tag{2.13}$$

The mapping procedure gives a full three-dimensional description of this ring-like structure. All the material parameters are mapped by the mapping function and hence they follow the experimental informations about geometry and composition of the structure. We can then solve the corresponding exciton problem to find the excitonic energy and corresponding wave function using the above position-dependent parameters.

2.3 Exact-diagonalization of the Excitonic Hamiltonian

To obtain the excitonic energy and wave function of the system we implement the exact-diagonalization method [15, 16]. This method uses the non-interacting electron and hole wave functions as basis to expand the excitonic wave function and then diagonalize the excitonic Hamiltonian.

The exciton Hamiltonian is expressed as:

$$\widehat{H}_X = \widehat{H}_e + \widehat{H}_h - e^2 G(\mathbf{r}_e, \mathbf{r}_h), \tag{2.14}$$

where $G(\mathbf{r}_e, \mathbf{r}_h)$ is the Green's function of the Poisson equation

$$\epsilon_0 \boldsymbol{\nabla}_\mathbf{r} \left[\epsilon(\mathbf{r}) \boldsymbol{\nabla}_\mathbf{r} G(\mathbf{r}, \mathbf{r}') \right] = -\delta(\mathbf{r} - \mathbf{r}'), \tag{2.15}$$

$\epsilon(\mathbf{r})$ is the position dependent permittivity defined in previous section, $\widehat{H}_e$ and $\widehat{H}_h$ are the non-interacting electron and hole Hamiltonians:

$$\widehat{H}_{e(h)} = \frac{1}{2} \boldsymbol{\Pi}_\mathbf{r}^{e(h)} \left(\frac{1}{m_{e(h)}^*(\mathbf{r})} \right) \boldsymbol{\Pi}_\mathbf{r}^{e(h)} + V_{e(h)}(\mathbf{r}), \tag{2.16}$$

where $\mathbf{V}_{e(h)}(\mathbf{r})$ and $\mathrm{m}_{e(h)}^*(\mathbf{r})$ are the electronic (hole) confinement potential and effective mass, $\boldsymbol{\Pi}_\mathbf{r}^{e(h)} = -i\hbar\nabla_\mathbf{r} + (-)e\mathbf{A}(\mathbf{r})$ is the momentum operator for electron (hole), $\mathbf{A}(\mathbf{r})$ is the vector potential of the magnetic field $\mathbf{B}(\mathbf{r}) = \nabla \times \mathbf{A}(\mathbf{r})$ and e is the absolute value of electron charge. We ignore the electron and hole spins in this study. Solving the above non-interacting problems we obtain the vector spaces for electron and hole $\Lambda_e(\mathbf{r}_e)$ and $\Lambda_h(\mathbf{r}_h)$ which are spanned by the non-interacting electron and hole basis $\{F_{el}(\mathbf{r}_e)\}$ and $\{F_{hk}(\mathbf{r}_h)\}$, where el and hk represent the main quantum numbers of the electron and hole. The excitonic wave function can be expanded by the non-interacting electron and hole basis:

$$\Psi_X(\mathbf{r}_e, \mathbf{r}_h) = \sum_i a_i \left[\Lambda_e(\mathbf{r}_e) \otimes \Lambda_h(\mathbf{r}_h) \right], \tag{2.17}$$

where i indicates the set of certain possible transitions: $\{el; hk\}$. We obtain the excitonic energy E_X from the following secular equation

$$\det \left[(E_{el} + E_{hk} + E_{g,in} - E_X) \, \delta_{ij} - e^2 G_{ij} \right] = 0. \tag{2.18}$$

The coefficient a_i can be obtained from:

$$\sum_j \left\{ (E_{el} + E_{hk} + E_{g,in}) \, \delta_{ij} - e^2 G_{ij} \right\} \cdot a_j = E_X^n \cdot a_i, \tag{2.19}$$

where

$$G_{ij} = \int F_{el} \left(\mathbf{r}_e \right) F_{el'} \left(\mathbf{r}_e \right) V_{hk;hk'}(\mathbf{r}_e) d\mathbf{r}_e, \tag{2.20}$$

and we can possess $V_{hk;hk'}(\mathbf{r}_e)$ by solving the Poisson equations for all sets $\{hk, hk'\}$:

$$\epsilon_0 \nabla_{\mathbf{r}} \left[\epsilon \left(\mathbf{r} \right) \nabla_{\mathbf{r}} V_{hk;hk'}(\mathbf{r}) \right] = -F_{hk} \left(\mathbf{r} \right) F_{hk'}(\mathbf{r}). \tag{2.21}$$

2.4 Definition of the Diamagnetic Shift Coefficients

To calculate the diamagnetic shift we choose the following gauges for the vector potential [17]:
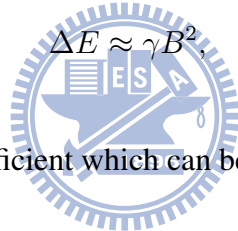
$$\mathbf{A}(\mathbf{r_e}) = \frac{1}{2}\mathbf{B} \times (\mathbf{r}_e - \overline{\mathbf{r_e}}); \quad \mathbf{A}(\mathbf{r_h}) = \frac{1}{2}\mathbf{B} \times (\mathbf{r}_h - \overline{\mathbf{r_e}}), \tag{2.22}$$

where $\overline{\mathbf{r_e}} = (\overline{x_e}, \overline{y_e}, \overline{z_e})$ and $\overline{\mathbf{r_h}} = (\overline{x_h}, \overline{y_h}, \overline{z_h})$ with

$$
\begin{aligned}
\overline{x_e} &= \langle \psi_X | x_e | \psi_X \rangle; \tag{2.23} \\
\overline{y_e} &= \langle \psi_X | y_e | \psi_X \rangle; \\
\overline{z_e} &= \langle \psi_X | z_e | \psi_X \rangle; \\
\overline{x_h} &= \langle \psi_X | x_h | \psi_X \rangle; \\
\overline{y_h} &= \langle \psi_X | y_h | \psi_X \rangle, \\
\overline{z_h} &= \langle \psi_X | z_h | \psi_X \rangle,
\end{aligned}
$$

those are the expectation values of the electron and hole positions.

With the above gauges in the low-field limit and $\mathbf{B}$ applied in the z-direction we can approximate the energy shift of the exciton in ground state as

$$
\Delta E \approx \gamma B^2, \tag{2.24}
$$

where γ is the diamagnetic shift coefficient which can be calculated through

$$
\frac{e^2}{8} \left(\langle \frac{(x - \overline{x_e})^2 + (y - \overline{y_e})^2}{m_e^*} \rangle + \langle \frac{(x - \overline{x_h})^2 + (y - \overline{y_h})^2}{m_h^*} \rangle \right). \tag{2.25}
$$

The numerator of the expectation values in Eq. (3.15) is the effective extension for the electron and hole confined in the ring, and thus corresponds to the actual lateral confinement of the exciton. Thus by calculating γ we can possess the knowledge of the distribution of the excitonic wave function and actual position of the exciton in this system.

2.5 Mesh Grids and the Calculation Details

The mesh grids is important in this simulation since there is two equaled valleys while using a mathematical model. The ground state wave function of a particle confined in the potential

with two balanced valleys is expected to extend into the both potential valleys equivalently. According to our computation experiences, if the density of the mesh is inadequate or not following the reflectional symmetry the calculated wave function of the particle will not reveal such symmetry.

We build the model of the ring using COMSOL multiphysics package (www.comsol.com). This package can generate meshes automatically and conveniently, but the meshes produced are not always decent and balanced for a full three dimensional calculation. While solving our problem in ideal situation we should have a mesh with infinitesimal distance between every two mesh points so a exact result can be obtained. However, practically due to machine power and memory limitations we can only produce a mesh with distances between every two mesh points as small as possible to reduce the error. In this study we monitor the error which comes from mesh by looking into the terms of (2.20). For example, due to a reflectional symmetry (while there are no structural imperfections) the term

$$G_{12} = \int F_{e1}\left(\mathbf{r}_e\right) F_{e2}\left(\mathbf{r}_e\right) V_{h1;h1}(\mathbf{r}_e) d\mathbf{r}_e = 0. \tag{2.26}$$

Since $F_{e1}(\mathbf{r_e})$ and $V_{h1;h1}(\mathbf{r_r})$ are even functions and $F_{e2}(\mathbf{r_e})$ is odd (the potential is an even function due to reflectional symmetry, so the ground state of the particle in the potential is even and the first excited state is odd), ideally the above term should be zero. However, if we use the mesh produced automatically by the package with only 59,711 mesh points the value of the term is in an order of 10^{-7} eV which is close to the energy diamagnetic shift with an order of 10^{-6} eV in low magnetic field. Therefore, an error rises while the mesh is not appropriately defined.

There are two possible ways to eliminate the error caused by the mesh. The first one is by increasing the mesh size, thus the distance between mesh points decreases. But at the same time requirements for machine power and memory are getting to physical machine limits. If the mesh is generated with an upper bound of 1.02 nm for the distance between two mesh points in the central part of the simulation domain, the calculated electron and hole wave function can distributed into both potential valleys equally. Nevertheless, the mesh with 219,009 mesh points

11

in total can only be used to calculate electron and hole separately, because of the limitation of the machine memory we can not involve enough large number of electron and hole states to expand the excitonic wave function for our a system. Hence we choose an adaptive mesh grids as shown in Fig. 2.3. The distance between mesh points in the central part within a region 50nm×40nm×20 nm is 1.25nm. This mesh follows the symmetry of the system and minimizes the disbalance in the particles' wave function with the value of (2.26) reduced to an order of 10^{-15} eV which gives a good accuracy. We shorten the length of the outside domain (relative to the center part) to reduce the requirement of machine power. The particles' wave functions are localized in the central part and they are more extended in x-direction than in y-direction, thus decreasing the domain length in y-direction causes only negligible errors. For consistency of this work we keep the same mesh upon changing the value of Δh and ΔV. The simulation is performed within a domain with edges 120nm×80nm×80nm with 92,169 mesh points in total.

In this study we take five electronic states and five hole states to expand the exciton wave function since there are only five electron states confined in the system while the structural imperfections are not included. We find the convergence by keeping the same number of electron states and increasing the number of hole states. The difference of the exciton ground state energy when we take five hole states or four hole states to expand the exciton wave function is only in an order of 10^{-7} eV. Therefore, we take five hole states as well. In order to maintain a consistency in this work we keep the same computational configuration while varying the values of Δh and ΔV.
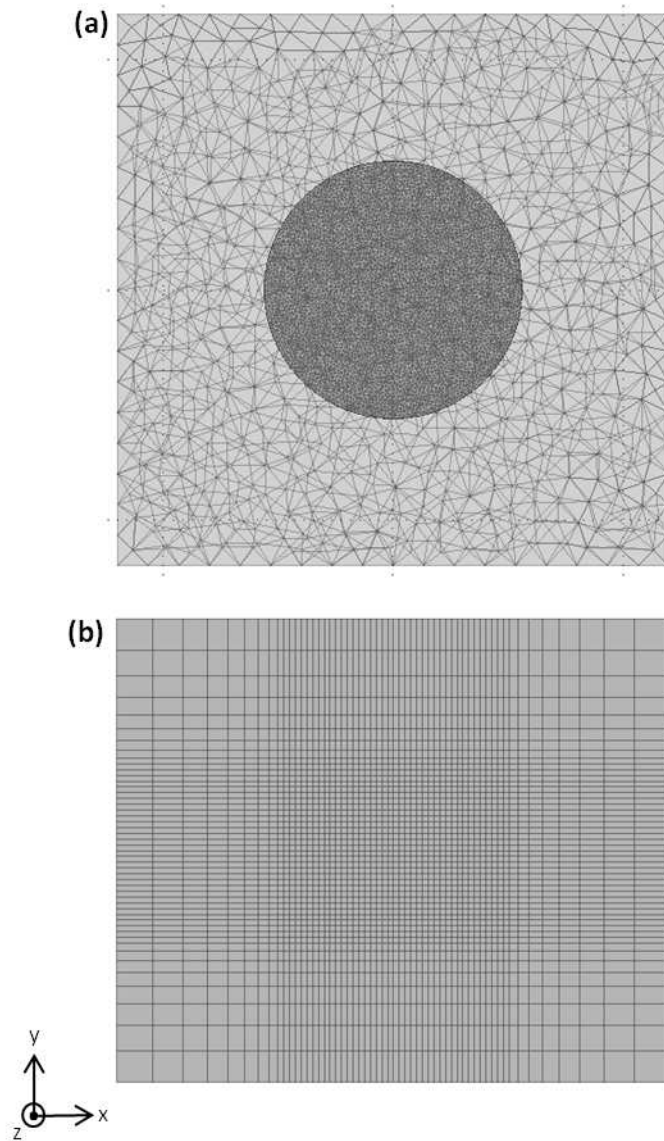
Figure 2.3: Top view of the meshes. (a) The mesh is generated randomly by COMSOL multi-physics package with 219,009 mesh points. (b) The mesh is controlled and used in our simulation with 92,169 mesh points.

13

Chapter 3

Results and Discussion

We use the parameters for the height profile as suggested in Ref. [12] and c = 0.55 is chosen to be the indium content in the $In_cGa_{1-c}As$ quantum ring. Material parameters such as effective masses, band gaps for electron and hole in strained *InAs* is taken from Ref. [13]. All values of the parameters are listed in Table 3.1. m_0 stands for the electron rest mass and ϵ_0 is the permittivity in vacuum.

The structural imperfections are included in this work by considering ΔV = -0.2, -0.1, 0, 0.1, 0.2 (we use (2.8) while ΔV=0 and (2.10) when $\Delta V \neq 0$) and Δh = -20%, -10%, 0%, 10%, 20% with appropriate sets of {a_{in}, a_{out}} listed in Table 3.2. While varying Δh both the geometry and the confinement potential alter (see Fig. 3.1 and 3.2). Changes in the confinement potential due to changes of ΔV is depicted in Fig. 3.2(d) and 3.2(e). In Fig. 3.3 we present the electronic confinement potentials with both Δh and ΔV varying.

From our simulation we found that when the potential is symmetric about x=0 plane the exciton wave function are distributed equally within two valleys of the potential at the ring's rim. However, when we induce small variations in either the ring's geometry or the potential the wave function collapses into one of the valleys, as a consequence, the spread of the probability distribution of the exciton shrinks.

Fig. 3.4 demonstrates the probability density of the excitons confined in the quantum ring. While there is no wobbling asymmetry the wave function extends to both valleys equally (see Fig. 3.4(a)). If we impose a structural imperfection either by decreasing Δh or ΔV with 10% of their original value the exciton tends to be stay in the valley on the negative x side (Fig. 3.4(b)). If we increase each of Δh or ΔV the wave function of the exciton collapses into another valley (Fig. 3.4(c)).

Table 3.1: Values of parameters used in this study.

Parameter	Value	Parameter	Value
$^\dagger m^*_{e,in}$	0.054 m_0	R	10.75 nm
$m^*_{e,out}$	0.067 m_0	γ_0	3 nm
$^\dagger m^*_{h,in}$	0.266 m_0	γ_∞	3 nm
$m^*_{h,out}$	0.500 m_0	h_M	3.6 nm
$^\dagger E_{g,in}$	0.147 eV	h_0	1.6 nm
$E_{g,out}$	1.159 eV	h_∞	0.4 nm
$^\dagger \Delta E$	0.230 eV	ξ	0.2
$^\dagger \epsilon_{in}$	14.138 ϵ_0	ξ_γ	-0.25
ϵ_{out}	12.900 ϵ_0	ξ_R	0.07
x_p	11.5 nm	b	6 nm
y_p	0 nm	b_V	4 nm
x_V	18.5 nm		

†Parameters inside the $In_cGa_{1-c}As/GaAs$ ring
 are taken by interpolation.

Table 3.2: Parameters for asymmetries.

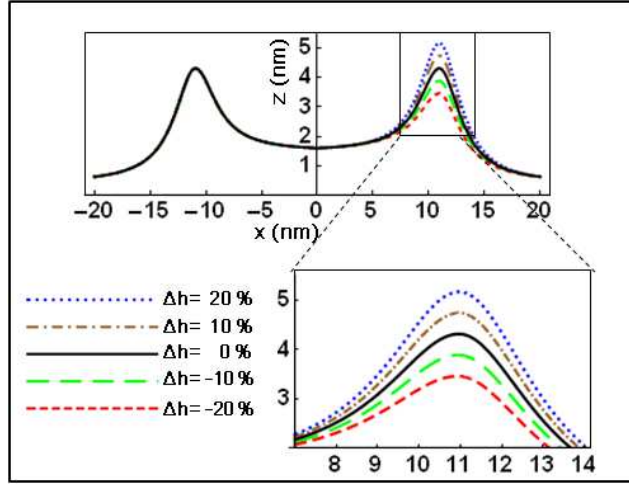| $\Delta h(\%)$	Parameter	Value
-20	a_{in}	-0.3180
	a_{out}	-0.2206
-10	a_{in}	-0.1590
	a_{out}	-0.1103
0	a_{in}	0.0000
	a_{out}	0.0000
+10	a_{in}	0.1590
	a_{out}	0.1103
+20	a_{in}	0.3180
	a_{out}	0.2206

15

Figure 3.1: The ring's height profiles with different Δh. The ring's heights are unchanged along the negative x-direction.

We know that the diamagnetic shift coefficient (γ) is proportional to the effective area spanned by the exciton wave function, therefore, if the extension of the exciton wave function decreases the coefficient drops as well. We define $\gamma(\Delta h, \Delta V)$ as a function of the parameters Δh and ΔV and present with the ratio of $\gamma(\Delta h, \Delta V)$ to $\gamma(0,0)$. We calculate γ with varying only one parameter for the structural imperfection and the ratio is shown in table 3.3. The result demonstrates that with either a small variation in the wobbling asymmetry or a small disbalanced potential lead to decrease of γ. In table 3.4 we show the ratio while both the wobbling asymmetry and the disbalanced potential are considered, and we obtain the same tendency for γ.
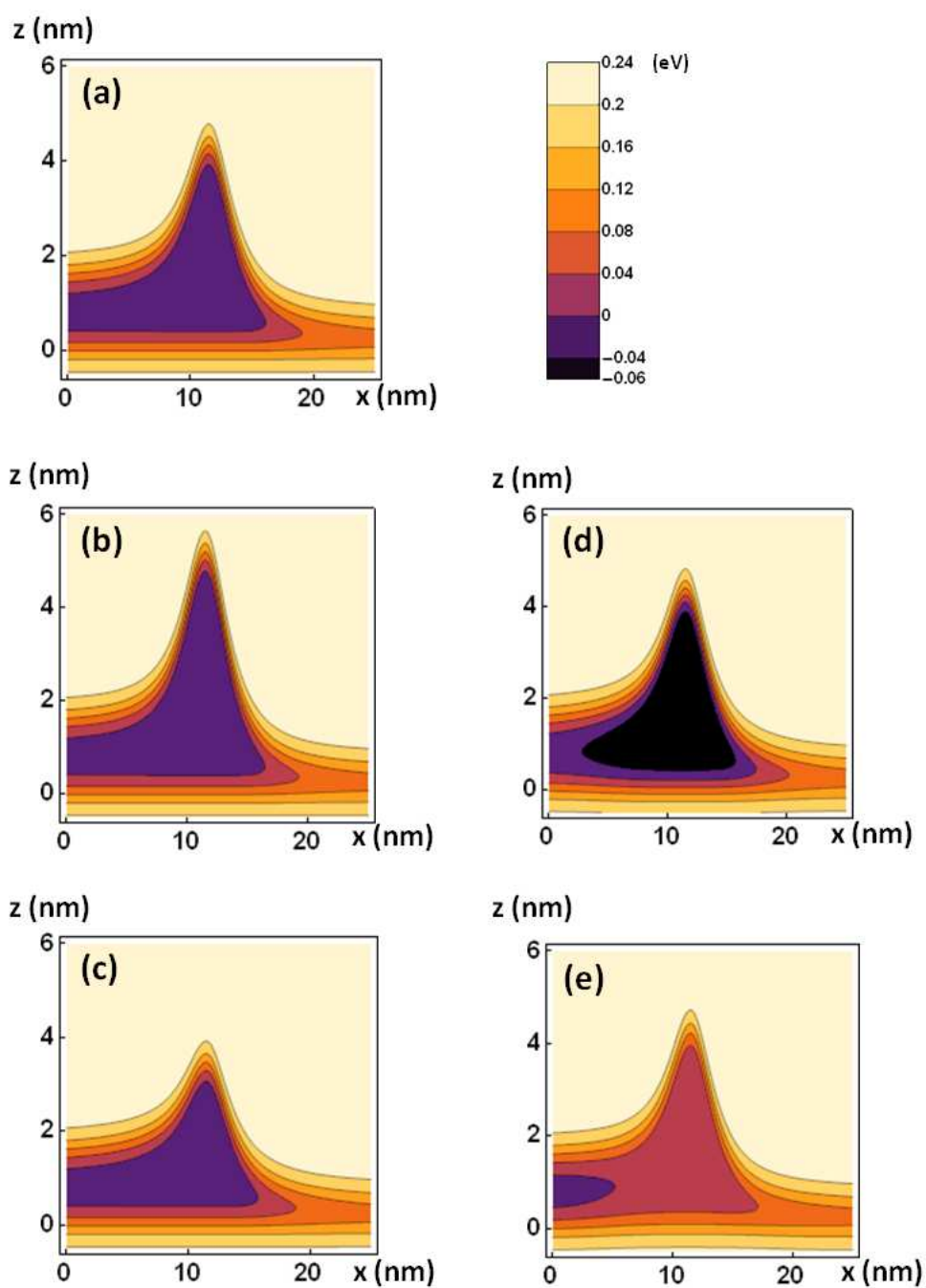
Figure 3.2: Projections of the electronic confinement potential onto x-z plane, the positive x direction is shown. (a): potential of a symmetrically wobbled ring; (b): Δh=20%, ΔV=0; (c): Δh=-20%, ΔV=0; (d): Δh=0%, ΔV=0.2; (e): Δh=0%, ΔV=-0.2.
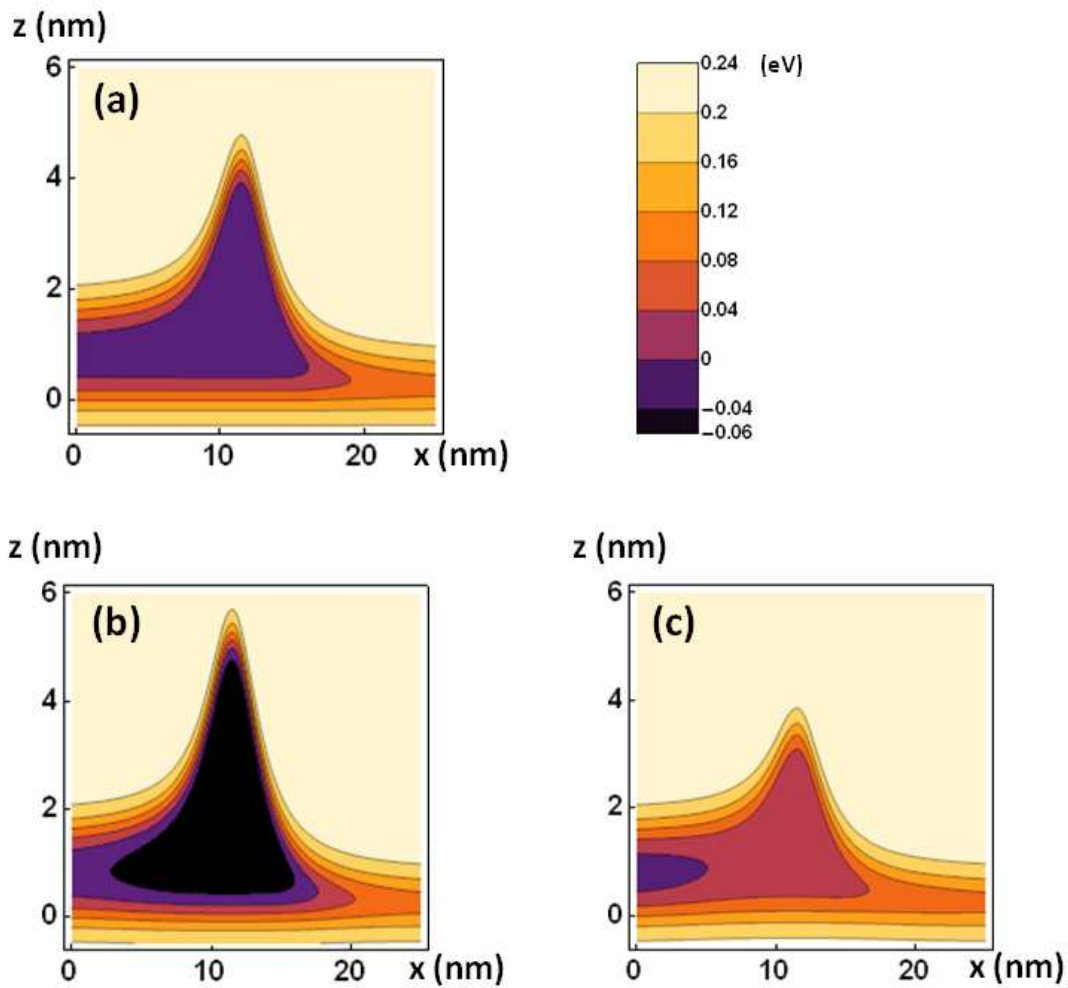
Figure 3.3: Projections of electronic potential on x-z plane changing both Δh and ΔV. (a): $\Delta h = \Delta V = 0$; (b): Δh=20%, ΔV=0.2; (c): Δh=-20%, ΔV=-0.2.
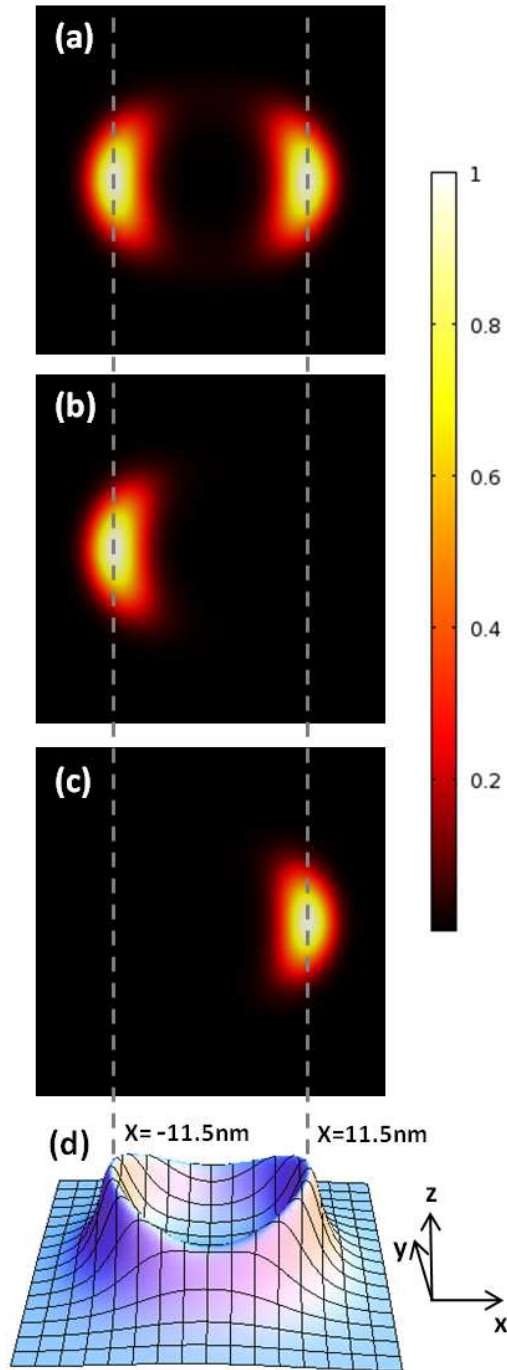
Figure 3.4: Probability densities for the excitons confined in nano-rings, projected onto the x-y plane with (a) $\Delta h = \Delta V = 0$, (b) Δh = -10% and ΔV = -0.1 and (c) Δh = 10% and ΔV = 0.1. (d) the height profile of a symmetrically wobbled ring and gives a reference for the location of the exciton probability densities. The dashed lines indicate the position at x = 11.5nm and x = -11.5nm.

Table 3.3: Normalized coefficients of energy diamagnetic shift as a function on Δh and ΔV.

| $\Delta h(\%)$	$\gamma(\Delta h, 0)/\gamma(0,0)$	ΔV	$\gamma(0, \Delta V)/\gamma(0,0)$
-20	0.32	-0.2	0.31
-10	0.35	-0.1	0.32
0	1.00	0	1.00
10	0.29	0.1	0.29
20	0.28	0.2	0.27

Table 3.4: Normalized coefficients of energy diamagnetic shift while changing both Δh and ΔV.

$(\Delta h, \Delta V)$	$\gamma(\Delta h, \Delta V)/\gamma(0,0)$
(-20%, -0.2)	0.33
(-10%, -0.1)	0.35
(0%, 0)	1.00
(10%, 0.1)	0.26
(20%, 0.2)	0.23

Notice that when we decrease either Δh or ΔV, the ratio $\gamma(\Delta h, \Delta V)/\gamma(0,0)$ approaches 0.3. Because for those changes the excitonic wave functions are located at the unchanged potential valley, the effective areas spanned by the excitonic wave functions are similar no matter which parameter we decrease. The same results appear while we decrease both the parameters simultaneously (see table 3.4), which supports our arguments. However, if Δh and ΔV continue increasing γ keeps dropping. When we enhance both Δh and ΔV to 20% and 0.2 respectively the ratio $\gamma(\Delta h, \Delta V)/\gamma(0,0)$ approaches 0.23 and the calculated excitonic energy diamagnetic shift coefficient reaches 10 $\mu eV/T^2$. The reason for the minification of γ is that the confinement is stronger when imposing two kinds of imperfections than considering only one of them, thus the extension of the exciton wave function is more restricted inside the valley which the structural imperfections are applied. The result conforms with the experimental measurement of a averaging value of 6.8 $\mu eV/T^2$ [9].

The calculated excitonic ground state energies are shown in Fig. 3.5 and Fig. 3.6. With a symmetrically wobbled ring and balanced confinement potential the excitonic ground state en-

ergy is about 1360 meV which is higher compared with the energies when imperfections are applied. The coulombic interaction between electron and hole is smaller due to a wider extension of excitonic wave function when the excitonic wave function is distributed into both potential valleys, therefore the excitonic ground state energy is higher. If we impose structural imperfections the excitonic ground state energy would go down because now the exciton is located in one of the potential valleys and the coulombic interaction is stronger because of a reduced extension of the excitonic wave functions. While we decrease either Δh or ΔV the energies reach 1350 meV (see Fig. 3.5 and 3.6). Because the excitons stay now in the unchanged potential valley, the energies saturate while the degree of the imperfections become larger. However, when the imperfections are imposed involving a raise of ΔV the exciton ground state energies continue dropping. Since in this situation the exciton locates in the valley where the potential depth is decreasing, the excitonic energies are dropping as ΔV increasing. The calculated excitonic ground state energies range from 1300 meV to 1340 meV while disbalanced potentials are imposed and the results consist with the experimental measurement of 1320 meV [9].
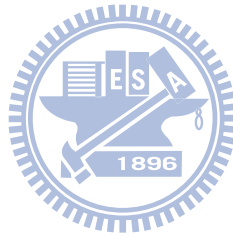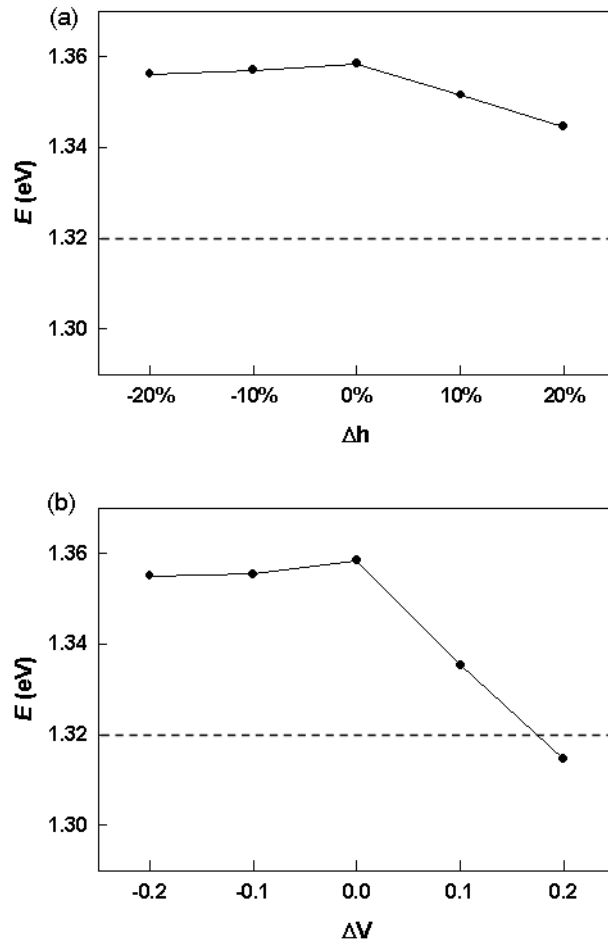
Figure 3.5: The excitonic transition energies with different (a) Δh and (b) ΔV. The dashed lines indicate the experimental measurement of excitonic energy: 1320 meV.
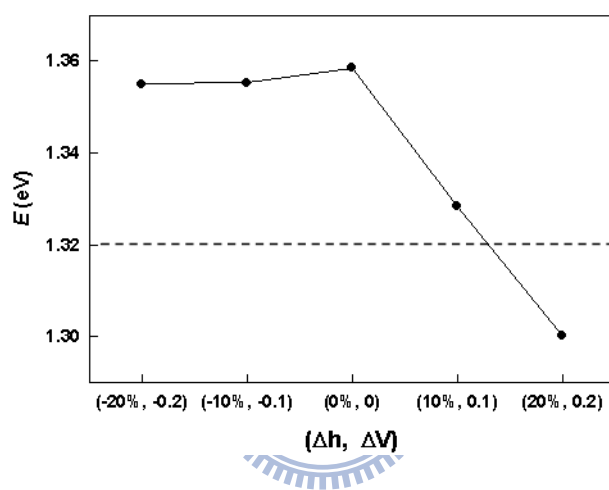
Figure 3.6: The excitonic transition energies when changing simultaneously both Δh and ΔV. The dashed line indicates the experimental measurement of excitonic energy: 1320 meV.

Chapter 4

Conclusion and Future Work

4.1 Conclusion

In conclusion, we calculate the excitonic diamagnetic shift coefficients of wobbled and singly-connected *InAs/GaAs* semiconductor nano-rings using the mapping and exact-diagonalization methods. Beside a mathematically model with a reflectional symmetry in the confinement potential we introduce two possible structural imperfections - wobbling asymmetry and disbalanced potentials - in our simulation. Within these approaches and taking an appropriate mesh we are able to describe this system. From our simulation we found that with small deviations in the geometries and confinement potentials the excitonic diamagnetic shift coefficient decreases greatly. Our results are in a good agreement with the experimental measurings.
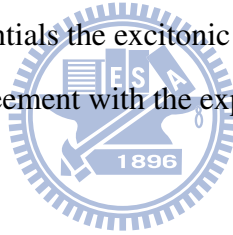
4.2 Previous Works

In Ref. [18] we calculated the excitonic and biexcitonic energies of *InAs/GaAs* nano-rings with geometry suggested in Ref. [8] and radius 7 nm. The problem was solved self-consistently using our mapping method, and we obtained preliminary results about this nano structure. After that we implemented the diagonalization method and calculated the magnetic response of rings in a weak magnetic field with an asymmetry in the geometry, this result was published in Ref. [19]. The magnetic susceptibility of wobbled semiconductor nano-rings were calculated in Ref. [20], and we found that the averaged susceptibility shows small temperature effect. The mapping method was used to calculate the energy of concentric triple nano-rings as well, and the calculated inhomogeneous broadening of the excitonic energy peaks was found in a good agreement with the experimental data [21].

4.3 Future Work

It is interesting to figure out the effect of structural imperfections on the diamagnetic shift coefficient of biexciton, and it can be compared with experimental measurement [9]. The reaction of charged excitons such as X^+ and X^- (exciton with an extra electron or a hole) in the system with applying the imperfections is worth studying as well.
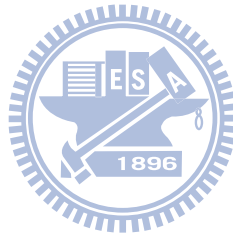
References

[1] Y. Aharonov and D. Bohm, "Significance of Electromagnetic Potentials in the Quantum Theory," *Physical Review* **115**, 485 (1959).

[2] A. Lorke, R. J. Luyken, A. O. Govorov, J. P. Kotthaus, J. M. García and P. M. Petroff, "Spectroscopy of Nanoscopic Semiconductor Rings," *Physical Review Letters* **84**, 2223 (2000).

[3] A. Fuhrer, S. Lüscher, T. Ihn, T. Heinzel, K. Ensslin, W. Wegscheider and M. Bichler, "Energy spectra of quantum rings," *Nature (London)* **413**, 822 (2001).

[4] O. Voskoboynikov, Y. Li, H. -M. Lu, C -F. Shih, and C. P. Lee, "Energy states and magnetization in nanoscale quantum rings," *Physical Review B* **66**,155306 (2002).

[5] M. Aichinger, S. A. Chin, E. Krotscheck, and E. Räsänen, "Effects of geometry and impurities on quantum rings in magnetic fields," *Physical Review B* **73**, 195310 (2006).

[6] O. Voskoboynikov, C. M. J. Wijers, J. L. Liu, and C. P. Lee, "Magneto-optical response of layers of semiconductor quantum dots and nanorings," *Physical Review B* **71**, 245332 (2005).

[7] D. Haft, C. Schulhauser, A. O. Govorov, R. J. Warburton, K. Karrai, J. M. Garcia, W. Schoenfeld, P. M. Petroff, "Magneto-optical properties of ring-shaped self-assembled InGaAs quantum dots," *Physica E* **13**, 165 (2002).

[8] P. Offermans, P. M. Koenraad, J. H. Wolter, D. Granados J. M. García, V. M. Fomin, V. N. Gladilin, and J. T. Devreese, "Atomic-scale structure of self-assembled InGaAs quantum rings in GaAs," *Applied Physics Letters* **87**, 131902 (2005).

[9] T. -C. Lin, C. -H. Lin, H. -S. Ling, Y. -J. Fu, W. -H. Chang, S. -D. Lin, and C. -P. Lee, "Impacts of structural asymmetry on the magnetic response of excitons and biexcitons in single self-assembled In(Ga)As quantum rings," *Physical Review B* **80**, 081304(R) (2009).

[10] S. N. Walck and T. L. Reinecke, "Exciton diamagnetic shift in semiconductor nanostructures," *Physical Review B* **57**, 9088 (1998).

[11] M. Grochol, F. Grose, and R. Zimmermann, "Exciton wave function properties probed by diamagnetic shift in disordered quantum wells," *Physical Review B* **71**, 125339 (2005).

[12] V. M. Fomin, V. N. Gladilin, S. N. Klimin, J. T. Devreese, N. A. J. M. Kleemans and P. M. Koenraad, "Theory of electron energy spectrum and Aharonov-Bohm effect in self-assembled $In_xGa_{1-x}As$ quantum rings in GaAs," *Physical Review B* **76**, 235320 (2007).

[13] C. E. Pryor and M. -E. Pistol, "Band-edge diagrams for strained III–V semiconductor quantum wells, wires, and dots," *Physical Review B* **72**, 205311 (2005).

[14] L. M. Thu and O. Voskoboynikov, *AIP Conference Proceedings* **1233**, 952 (2010).

[15] H. Hu, J. -L. Zhu, J. -J. Xiong, "Energy levels and far-infrared spectroscopy for two electrons in a nanoscopic semiconductor ring," *Physical Review B* **62**, 16777 (2000).

[16] L. M. Thu and O. Voskobonikov, "Magneto-optics of layers of double quantum dot molecules," *Physical Review B* **80**, 155442 (2009) .

[17] L. D. Landau and E. M. Lifshitz, "The Classical Theory of Fields," 4th revised English edition, *Pergamon Press Ltd* (1975).

[18] L. M. Thu, W. T. Chiu, Shao-Fu Xue, Ta-Chun Lin, and O. Voskoboynikov, "Binding energy of magneto-biexcitons in semiconductor nano-rings," *Physics Procedia* **3**, 1149 (2010).

[19] L. M. Thu, W. T. Chiu, Ta-Chun Lin, and O. Voskoboynikov, "Effect of geometry on the excitonic diamagnetic shift of nano-rings," accepted in *Physica Status Solidi C*, published online in 25 October 2010.

[20] L. M. Thu, W. T. Chiu, and O. Voskoboynikov, "Temperature stable positive magnetic susceptibility of semiconductor wobbled nano ring," *Journal of Physics: Conference Series* **245**, 012042 (2010).

[21] L. M. Thu, W. T. Chiu, and O. Voskoboynikov, "Inhomogeneous broadening of the excitonic peaks for ensembles of concentric triple nano-rings," submitted to *Physical Review B*.